

Dynamic energy enabled differentiation (DEED) image watermarking based on human visual system and wavelet tree classification

Min-Jen Tsai

Published online: 26 November 2009
© Springer Science + Business Media, LLC 2009

Abstract In this paper, we present a novel dynamic energy enabled differentiation (DEED) watermarking algorithm based on the wavelet tree classification and human visual system (HVS). The wavelet coefficients of the image are divided into disjoint trees and a wavelet tree consists of 21 coefficients which are divided into 6 blocks. One watermark bit is embedded into one wavelet tree using the energy differentiation of positive and negative modulation between coefficients of each block. In addition, the contrast sensitive function (CSF) of human visual system is also considered for better weighting in watermarking since the wavelet coefficients across the subbands perform different characteristics and importance. As DEED still requires extra storage of side information during the extraction and results non-blind watermarking approach, a random direction differentiation approach called DEED_R is then proposed which is a truly blind watermarking technique. This study has performed intensive comparison for the proposed scheme with other tree energy differentiation based techniques like WTQ, ABW-TMD and WTGM under various geometric and nongeometric attacks. From the experimental results, the advantage of DEED based algorithms is not only with low complexity, but also outperforms WTGM and WTQ in terms of robustness and imperceptibility of watermarking.

Keywords Digital image watermarking · Human visual system (HVS) · Tree energy differentiation · Wavelet

1 Introduction

As digital data are widely available online or elsewhere, and because they are easy to be modified, necessary works are required to protect the copyright and the verification of the

M.-J. Tsai (✉)

Institute of Information Management, National Chiao Tung University, 1001 Ta-Hsueh Road, Hsin-Chu 300 Taiwan, Republic of China
e-mail: mjsai@cc.nctu.edu.tw

embedded genuine information. Digital watermarking has received significant attraction recently due to the popularity of the Internet and demand for the ownership protection [3]. Among the techniques for watermarking [3–5, 9, 18, 19], the robustness of the digital watermarking is very crucial to counteract the various attacks of unauthorized modification.

Cox et al. [3] had proposed a global DCT-based spread spectrum approach to hide watermarks. Langelaar and Lagendijk [9] introduced the DEW (Differential Energy Watermarking) algorithm for JPEG/MPEG streams in the DCT domain. The DEW algorithm embeds label bits (the watermark) by selectively discarding high frequency DCT coefficients in certain image regions. Das, Maitra and Mitra had presented a successful cryptanalysis against the DEW scheme in [5] and proposed a more robust scheme.

On the other hand, Wang and Lin [18, 19] introduced the technique of WTQ (Wavelet Tree Quantization) in the wavelet domain. The wavelet coefficients are grouped into so called super trees. The wavelet tree based watermarking algorithm embeds watermark bits by selectively quantizing the super trees. Even if the attacker has no knowledge of which two trees are used for embedding, he can still quantize those super trees that are not quantized earlier with respect to the estimated quantization indices. Das and Maitra had presented how that can be accomplished in [4] and such cryptanalysis attack is also confirmed in this study.

Al-Otum and Samara [1] later proposed an adaptive blind wavelet watermarking technique using tree mutual difference called ABW-TMD where the total embedding error is minimized by investigating which tree pairs will be allowed to embed the watermark bit and the embedding position will be saved as a sequential value in a private key. Even this design shows superior results to resist various image processing attacks than WTQ, the existence of the private key containing the watermark embedding location indicates such watermarking technique can not be categorized as “blind” watermarking approach. The authors [1] may not be aware of such subtle difference and named their scheme blind but it actually is not.

Instead of only using the tree structure in the wavelet domain for image watermarking, tree group energy differentiation approach with the adoption of human visual system has been first proposed in WTGM [16, 17] algorithm. In WTGM, suppose that each watermark bit is embedded using one tree group, half of a tree group is used for positive modulation [10] and the other is used for negative modulation.

For suitable modulation, any two sub-tree groups should have close total energy (energy summation from wavelet tree coefficients) and the selection is essential the sum-of-subset problem in [5]. Even WTGM design is robust to the cryptanalysis of the watermarking attacks with high visual quality, the disadvantage for the WTGM is that the tree combination information must be kept secret which addresses extra storage space and the watermarking is not truly blind in essence. This is the similar situation from the analysis of ABW-TMD. Therefore, it is the motivation in this study to apply the dynamic energy enabled differentiation to investigate the differentiation approach with human visual system consideration for watermarking without the side information in this study. Under such conception, we proposed a human vision system based dynamic energy enabled differentiation (called DEED) watermarking algorithm which utilizes discrete wavelet transform (DWT) theory. DEED modifies the wavelet coefficient values of images dynamically and uses the differentiation of positive and negative modulation to embed the watermark. In the embedding process, we try to find the best coefficient energy differentiation direction of the embedded watermark

bit that make minimal change of coefficient's energy within the tree. We then change the wavelet tree coefficient energy dynamically with differentiation direction, and embed the designated watermark bits into the energy differentiation between the coefficients. The purpose of the DEED design is robust to the cryptanalysis of the watermarking attacks with high visual quality. The weakness of DEED is that the differentiation direction information should be recorded and extra storage of side information is required as the WTGM or ABW-TMD does, they can not be categorized as the blind watermarking approach which will be unsuitable in practical applications. Therefore, a random direction differentiation approach called DEED_R is then proposed which is a truly blind watermarking technique with high robustness against attacks.

Under such motivation, DEED and DEED_R can construct a better wavelet tree watermarking algorithm for digital images and offer more credible technique to protect the digital intellectual property rights. This paper will be organized as follows. The details of the algorithms will be explained in Section 2. Section 3 will show the experiments with discussion and conclusion is in Section 4.

2 The DEED approach and the algorithms

2.1 The watermark embedding of DEED

We employ the same wavelet tree structure as depicted in the WTQ scheme in Fig. 1. Suppose that a 512×512 image is transformed, each wavelet tree T will be a collection of 21 wavelet coefficients, one coefficient from level 4, 4 coefficients from level 3, and 16 coefficients from level 2, and we can get 3072 wavelet trees. That is, a 512×512 image will be decompose into 3072 wavelet tree T_n , where $0 \leq n \leq 3071$. We then divide the 21 coefficients of one tree into 6 blocks as shown in Fig. 2(a) and (b).

To embed the watermark into wavelet trees where the watermark sequence is a binary PN (± 1) sequence of watermark bits, the DEED algorithm tries to modify the coefficients in each block dynamically. Since there is only one coefficient for block one, the scalar quantization is applied for differentiation purpose. Therefore, one watermark bit is embedded in one tree by modifying the coefficient energy 6 times (one time for one block). We first quantize the coefficient of block 1 with a pre-defined modular value S , and the thresholds of differentiation T_1 and T_2 and the differentiation operations are as follows:

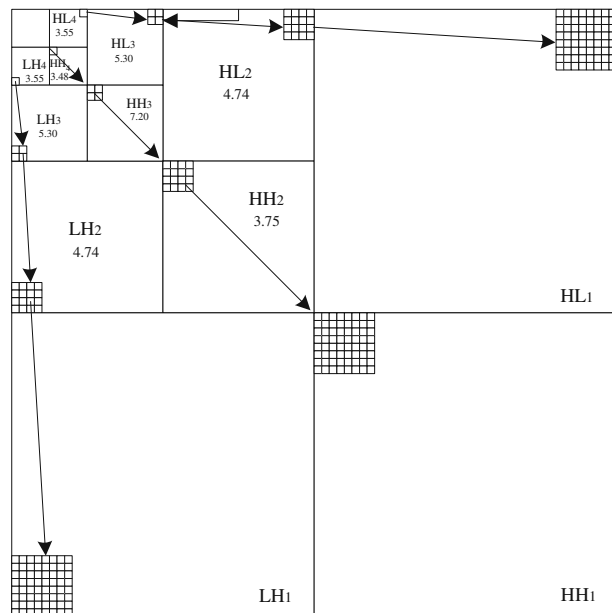
$$T_1 = \frac{S}{4}, \quad T_2 = \frac{3S}{4} \quad (1)$$

$$\delta_n(1) = T_n(1) \bmod S$$

$$T_n'(1) = \begin{cases} T_n(1) - \delta_n(1) + T_1, & \text{if } W_n = -1 \text{ and } T_n(1) \geq 0 \\ T_n(1) - \delta_n(1) + T_2, & \text{if } W_n = +1 \text{ and } T_n(1) \geq 0 \\ T_n(1) + \delta_n(1) - T_1, & \text{if } W_n = -1 \text{ and } T_n(1) < 0 \\ T_n(1) + \delta_n(1) - T_2, & \text{if } W_n = +1 \text{ and } T_n(1) < 0 \end{cases} \quad (2)$$

For block 2–6 which contains 4 coefficients in each block, DEED will adjust those coefficients according to the energy differentiation by positive and negative modulation.

Fig. 1 A four-level wavelet tree structure. The coefficients corresponding to the same spatial location are grouped together. Each tree consists of one coefficient from level 4, 4 coefficients from level 3, 16 coefficients from level 2. For WTGM (S_2) tree grouping, 64 coefficients from level 1 are adopted. The weighting values for each level k are indicated at the center of each band



First, we must determine a suitable differentiation direction of the block. There are 3 kinds of differentiation direction: vertical, horizontal and diagonal direction. If we can modify the energy of one block with different differentiation direction and make minimal change of the coefficients, the direction is exactly the best direction. Under such consideration, the best differentiation direction selection algorithm of wavelet coefficient energy is as follows:

Some notations are defined here for each tree T_n of group g , $1 \leq g \leq 5$, $0 \leq n \leq 3071$ and the length of watermark is N_w :

- $\sigma_{n,g}(U_r)$: The average of upper 2 coefficients
- $\sigma_{n,g}(L_r)$: The average of lower 2 coefficients
- $\sigma_{n,g}(L_t)$: The average of left 2 coefficients
- $\sigma_{n,g}(R_t)$: The average of right 2 coefficients
- $\sigma_{n,g}(D_1)$: The average of 2 left-diagonal coefficients
- $\sigma_{n,g}(D_2)$: The average of 2 right-diagonal coefficients

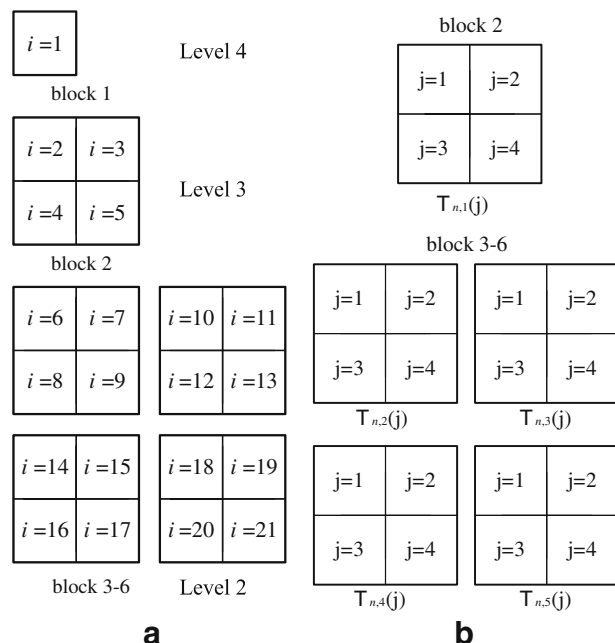
for ($n=0$; $n < N_w$; $n++$)

$$\left\{ \begin{array}{l} V_{n,g} = \sigma_{n,g}(U_r) - \sigma_{n,g}(L_r) \\ H_{n,g} = \sigma_{n,g}(L_t) - \sigma_{n,g}(R_t) \\ D_{n,g} = \sigma_{n,g}(D_1) - \sigma_{n,g}(D_2) \end{array} \right. \quad (3)$$

if ($w_n == -1$)

$$\text{direction}_{n,g} = \text{find_maximum}(V_{n,g}, H_{n,g}, D_{n,g})$$

Fig. 2 a There are 21 coefficients to form a tree which is divided into 6 blocks. **b** In block 2–6, 4 nearby coefficients in level 2 and 3 are grouped to form blocks. The symbol $T_{n,g}(j)$ represents the coefficient in tree T_n of group g , $1 \leq g \leq 5$ and $1 \leq j \leq 4$



else if ($w_n == 1$)

$$\text{direction}_{n,g} = \text{find_minimum}(\mathbf{V}_{n,g}, \mathbf{H}_{n,g}, \mathbf{D}_{n,g}) \}$$

Where $\text{direction}_{n,g}=0,1,2$ means the differentiation direction is vertical, horizontal or diagonal respectively for block g in tree T_n .

If we find the vertical direction is the best choice of the differentiation direction, we will first calculate the average value of upper and lower coefficients of block g of tree n :

$$\begin{cases} \sigma_{n,g}(Ur) = (T_{n,g}(1) + T_{n,g}(2))/2 \\ \sigma_{n,g}(Lr) = (T_{n,g}(3) + T_{n,g}(4))/2 \end{cases} \quad (4)$$

Then DEED will calculate the difference dif_v between $\sigma_{n,g}(Ur)$ and $\sigma_{n,g}(Lr)$ as

$$dif_v = |\sigma_{n,g}(Ur) - \sigma_{n,g}(Lr)| \quad (5)$$

After this step, DEED will adjust the coefficient values and the modified energy differentiation of $\sigma_{n,g}(Ur)$ and $\sigma_{n,g}(Lr)$ will become $\sigma'_{n,g}(Ur)$ and $\sigma'_{n,g}(Lr)$ which satisfy the following relationship:

$$\begin{cases} \sigma'_{n,g}(Ur) \geq \sigma'_{n,g}(Lr), & \text{if } w_n = -1 \\ \sigma'_{n,g}(Ur) < \sigma'_{n,g}(Lr), & \text{if } w_n = 1 \end{cases} \quad (6)$$

Let $E[\cdot]$ s represent the process of differential operations for each block coefficient. DEED will modify the coefficient energy to satisfy the conditions mentioned above:

$$\begin{cases} \begin{cases} E[T_{n,g}(j)] \\ \langle j = 1, 2 \rangle \\ W_n = -1 \end{cases} = \begin{cases} T_{n,g}(j) + \frac{\Delta}{2} & , \text{if } \sigma_{n,g}(Ur) = \sigma_{n,g}(Lr) \\ T_{n,g}(j) & , \text{if } \sigma_{n,g}(Ur) > \sigma_{n,g}(Lr) \text{ and } dif_v \geq \Delta \\ T_{n,g}(j) + \frac{\Delta - dif_v}{2} & , \text{if } \sigma_{n,g}(Ur) > \sigma_{n,g}(Lr) \text{ and } dif_v < \Delta \\ T_{n,g}(j) + \frac{dif_v + \Delta}{2} & , \text{if } \sigma_{n,g}(Ur) < \sigma_{n,g}(Lr) \end{cases} \\ E[T_{n,g}(j)] \\ \langle j = 3, 4 \rangle \\ W_n = -1 \end{cases} = \begin{cases} T_{n,g}(j) - \frac{\Delta}{2} & , \text{if } \sigma_{n,g}(Ur) = \sigma_{n,g}(Lr) \\ T_{n,g}(j) & , \text{if } \sigma_{n,g}(Ur) > \sigma_{n,g}(Lr) \text{ and } dif_v \geq \Delta \\ T_{n,g}(j) - \frac{\Delta - dif_v}{2} & , \text{if } \sigma_{n,g}(Ur) > \sigma_{n,g}(Lr) \text{ and } dif_v < \Delta \\ T_{n,g}(j) - \frac{dif_v + \Delta}{2} & , \text{if } \sigma_{n,g}(Ur) < \sigma_{n,g}(Lr) \end{cases} \\ \begin{cases} E[T_{n,g}(j)] \\ \langle j = 1, 2 \rangle \\ W_n = 1 \end{cases} = \begin{cases} T_{n,g}(j) - \frac{\Delta}{2} & , \text{if } \sigma_{n,g}(Ur) = \sigma_{n,g}(Lr) \\ T_{n,g}(j) & , \text{if } \sigma_{n,g}(Ur) < \sigma_{n,g}(Lr) \text{ and } dif_v \geq \Delta \\ T_{n,g}(j) - \frac{\Delta - dif_v}{2} & , \text{if } \sigma_{n,g}(Ur) < \sigma_{n,g}(Lr) \text{ and } dif_v < \Delta \\ T_{n,g}(j) - \frac{dif_v + \Delta}{2} & , \text{if } \sigma_{n,g}(Ur) > \sigma_{n,g}(Lr) \end{cases} \\ E[T_{n,g}(j)] \\ \langle j = 3, 4 \rangle \\ W_n = 1 \end{cases} = \begin{cases} T_{n,g}(j) + \frac{\Delta}{2} & , \text{if } \sigma_{n,g}(Ur) = \sigma_{n,g}(Lr) \\ T_{n,g}(j) & , \text{if } \sigma_{n,g}(Ur) < \sigma_{n,g}(Lr) \text{ and } dif_v \geq \Delta \\ T_{n,g}(j) + \frac{\Delta - dif_v}{2} & , \text{if } \sigma_{n,g}(Ur) < \sigma_{n,g}(Lr) \text{ and } dif_v < \Delta \\ T_{n,g}(j) + \frac{dif_v + \Delta}{2} & , \text{if } \sigma_{n,g}(Ur) > \sigma_{n,g}(Lr) \end{cases} \quad (7)$$

The Δ represents the differentiation intensity among the equations. When Δ is larger, the robustness of watermarking will be improved. In the mean time, it will affect the image quality more. While we have done the dynamic energy differentiation process from block 1 to block 6, the watermarking of bit w_n into tree T_n is completed. The differentiation direction of every tree must be recorded in a storage space.

For the differentiation in the horizontal or diagonal direction, the differentiation process is similar. We can replace Eq. 4–6 by Eq. 8–10 if the direction is horizontal and Eq. 11–13 if the direction is diagonal:

$$\begin{cases} \sigma_{n,g}(Lt) = (T_{n,g}(1) + T_{n,g}(3))/2 \\ \sigma_{n,g}(Rt) = (T_{n,g}(2) + T_{n,g}(4))/2 \end{cases} \quad (8)$$

$$Dif_h = |\sigma_{n,g}(Lt) - \sigma_{n,g}(Rt)| \quad (9)$$

$$\begin{cases} \sigma'_{n,g}(Lt) > \sigma'_{n,g}(Rt), & \text{if } w_n = -1 \\ \sigma'_{n,g}(Lt) < \sigma'_{n,g}(Rt), & \text{if } w_n = 1 \end{cases} \quad (10)$$

$$\begin{cases} \sigma_{n,g}(D_1) = (T_{n,g}(1) + T_{n,g}(4))/2 \\ \sigma_{n,g}(D_2) = (T_{n,g}(2) + T_{n,g}(3))/2 \end{cases} \quad (11)$$

$$Dif_d = |\sigma_{n,g}(D_1) - \sigma_{n,g}(D_2)| \quad (12)$$

$$\begin{cases} \sigma'_{n,g}(D_1) > \sigma'_{n,g}(D_2), & \text{if } w_n = -1 \\ \sigma'_{n,g}(D_1) < \sigma'_{n,g}(D_2), & \text{if } w_n = 1 \end{cases} \quad (13)$$

The Eq. 7 of energy differentiation calculation process could be replaced by Eq. 14 if the differentiation direction is horizontal and Eq. 15 if the direction is diagonal as follows:

$$\begin{aligned} \left\langle \begin{array}{l} E[T_{n,g}(j)] \\ j=1,3 \\ W_n = -1 \end{array} \right\rangle &= \begin{cases} T_{n,g}(j) + \frac{\Delta}{2} & , \text{if } \sigma_{n,g}(Lt) = \sigma_{n,g}(Rt) \\ T_{n,g}(j) & , \text{if } \sigma_{n,g}(Lt) > \sigma_{n,g}(Rt) \text{ and } dif_h \geq \Delta \\ T_{n,g}(j) + \frac{\Delta - dif_h}{2} & , \text{if } \sigma_{n,g}(Lt) > \sigma_{n,g}(Rt) \text{ and } dif_h < \Delta \\ T_{n,g}(j) + \frac{dif_h + \Delta}{2} & , \text{if } \sigma_{n,g}(Lt) < \sigma_{n,g}(Rt) \end{cases} \\ \left\langle \begin{array}{l} E[T_{n,g}(j)] \\ j=2,4 \\ W_n = -1 \end{array} \right\rangle &= \begin{cases} T_{n,g}(j) - \frac{\Delta}{2} & , \text{if } \sigma_{n,g}(Lt) = \sigma_{n,g}(Rt) \\ T_{n,g}(j) & , \text{if } \sigma_{n,g}(Lt) > \sigma_{n,g}(Rt) \text{ and } dif_h \geq \Delta \\ T_{n,g}(j) - \frac{\Delta - dif_h}{2} & , \text{if } \sigma_{n,g}(Lt) > \sigma_{n,g}(Rt) \text{ and } dif_h < \Delta \\ T_{n,g}(j) - \frac{dif_h + \Delta}{2} & , \text{if } \sigma_{n,g}(Lt) < \sigma_{n,g}(Rt) \end{cases} \\ \left\langle \begin{array}{l} E[T_{n,g}(j)] \\ j=1,3 \\ W_n = 1 \end{array} \right\rangle &= \begin{cases} T_{n,g}(j) - \frac{\Delta}{2} & , \text{if } \sigma_{n,g}(Lt) = \sigma_{n,g}(Rt) \\ T_{n,g}(j) & , \text{if } \sigma_{n,g}(Lt) < \sigma_{n,g}(Rt) \text{ and } dif_h \geq \Delta \\ T_{n,g}(j) - \frac{\Delta - dif_h}{2} & , \text{if } \sigma_{n,g}(Lt) < \sigma_{n,g}(Rt) \text{ and } dif_h < \Delta \\ T_{n,g}(j) - \frac{dif_h + \Delta}{2} & , \text{if } \sigma_{n,g}(Lt) > \sigma_{n,g}(Rt) \end{cases} \\ \left\langle \begin{array}{l} E[T_{n,g}(j)] \\ j=2,4 \\ W_n = 1 \end{array} \right\rangle &= \begin{cases} T_{n,g}(j) + \frac{\Delta}{2} & , \text{if } \sigma_{n,g}(Lt) = \sigma_{n,g}(Rt) \\ T_{n,g}(j) & , \text{if } \sigma_{n,g}(Lt) < \sigma_{n,g}(Rt) \text{ and } dif_h \geq \Delta \\ T_{n,g}(j) + \frac{\Delta - dif_h}{2} & , \text{if } \sigma_{n,g}(Lt) < \sigma_{n,g}(Rt) \text{ and } dif_h < \Delta \\ T_{n,g}(j) + \frac{dif_h + \Delta}{2} & , \text{if } \sigma_{n,g}(Lt) > \sigma_{n,g}(Rt) \end{cases} \end{aligned} \quad (14)$$

$$\begin{aligned} \left\langle \begin{array}{l} E[T_{n,g}(j)] \\ j=1,4 \\ W_n = -1 \end{array} \right\rangle &= \begin{cases} T_{n,g}(j) + \frac{\Delta}{2} & , \text{if } \sigma_{n,g}(D_1) = \sigma_{n,g}(D_2) \\ T_{n,g}(j) & , \text{if } \sigma_{n,g}(D_1) > \sigma_{n,g}(D_2) \text{ and } dif_d \geq \Delta \\ T_{n,g}(j) + \frac{\Delta - dif_d}{2} & , \text{if } \sigma_{n,g}(D_1) > \sigma_{n,g}(D_2) \text{ and } dif_d < \Delta \\ T_{n,g}(j) + \frac{dif_d + \Delta}{2} & , \text{if } \sigma_{n,g}(D_1) < \sigma_{n,g}(D_2) \end{cases} \\ \left\langle \begin{array}{l} E[T_{n,g}(j)] \\ j=2,3 \\ W_n = -1 \end{array} \right\rangle &= \begin{cases} T_{n,g}(j) - \frac{\Delta}{2} & , \text{if } \sigma_{n,g}(D_1) = \sigma_{n,g}(D_2) \\ T_{n,g}(j) & , \text{if } \sigma_{n,g}(D_1) > \sigma_{n,g}(D_2) \text{ and } dif_d \geq \Delta \\ T_{n,g}(j) - \frac{\Delta - dif_d}{2} & , \text{if } \sigma_{n,g}(D_1) > \sigma_{n,g}(D_2) \text{ and } dif_d < \Delta \\ T_{n,g}(j) - \frac{dif_d + \Delta}{2} & , \text{if } \sigma_{n,g}(D_1) < \sigma_{n,g}(D_2) \end{cases} \\ \left\langle \begin{array}{l} E[T_{n,g}(j)] \\ j=1,4 \\ W_n = 1 \end{array} \right\rangle &= \begin{cases} T_{n,g}(j) - \frac{\Delta}{2} & , \text{if } \sigma_{n,g}(D_1) = \sigma_{n,g}(D_2) \\ T_{n,g}(j) & , \text{if } \sigma_{n,g}(D_1) < \sigma_{n,g}(D_2) \text{ and } dif_d \geq \Delta \\ T_{n,g}(j) - \frac{\Delta - dif_d}{2} & , \text{if } \sigma_{n,g}(D_1) < \sigma_{n,g}(D_2) \text{ and } dif_d < \Delta \\ T_{n,g}(j) - \frac{dif_d + \Delta}{2} & , \text{if } \sigma_{n,g}(D_1) > \sigma_{n,g}(D_2) \end{cases} \\ \left\langle \begin{array}{l} E[T_{n,g}(j)] \\ j=2,3 \\ W_n = 1 \end{array} \right\rangle &= \begin{cases} T_{n,g}(j) + \frac{\Delta}{2} & , \text{if } \sigma_{n,g}(D_1) = \sigma_{n,g}(D_2) \\ T_{n,g}(j) & , \text{if } \sigma_{n,g}(D_1) < \sigma_{n,g}(D_2) \text{ and } dif_d \geq \Delta \\ T_{n,g}(j) + \frac{\Delta - dif_d}{2} & , \text{if } \sigma_{n,g}(D_1) < \sigma_{n,g}(D_2) \text{ and } dif_d < \Delta \\ T_{n,g}(j) + \frac{dif_d + \Delta}{2} & , \text{if } \sigma_{n,g}(D_1) > \sigma_{n,g}(D_2) \end{cases} \end{aligned} \quad (15)$$

Even it is possible that an attacker can evaluate the difference between block coefficients to guess the watermarked bit if the tree decomposition structure is available through cryptanalysis approach of [4], DEED can resist such cryptanalysis attacks since the best differential direction among blocks are different. That is, the best differential directions among blocks are chosen based on the watermark bit and the

coefficient energy difference. Therefore, such dynamic selection provides the flexibility during the embedding. However, DEED will try to avoid the situation when all 6 blocks are decreased or increased in only one direction and the attackers might be able to compare with all other trees to extract the watermark bits and try to modify the tree coefficients to remove the watermark information.

Under such consideration, a more sophisticated design of watermarking is deployed during the embedding. A random number generator will be applied to select which group will embed the watermark bit w_n and the others will embed bit $-w_n$. For example, if $g=1,2,4$ are selected for tree T_n to embed bit w_n , group 3,5 will embed bit $-w_n$. Such arrangement will confuse the attackers since they can not find consistent embedding direction and no way to extract or remove the watermarks.

2.2 The watermark extraction of DEED

To extract the watermark from wavelet trees, the DEED algorithm must get the 6 possible outcomes of watermark bit w'_n from block 1 to block 6 for reconstructed wavelet tree T'_n . After the information is collected, DEED can determine the final value of w'_n from the 6 outcomes. If $D[\cdot]$ means the process of watermark extraction, we extract the possible w'_n from block 1 as follows:

$$\theta_n(1) = T'_n(1) \mod S \quad (16)$$

$$D[T'_n(1)] = \begin{cases} -1 & , \text{if } |\theta_n(1)| < \frac{T_1+T_2}{2} \\ +1 & , \text{if } |\theta_n(1)| \geq \frac{T_1+T_2}{2} \end{cases} \quad (17)$$

We then need to extract the embedding information from block 2–6 by comparison of differentiation direction and coefficient energy. If $d(T_{n,g})=0,1,2$ means the differentiation direction is vertical, horizontal or diagonal of block g in T_n , the equations of watermark extraction as follows:

$$\begin{aligned} D[T'_{n,g}] &= \begin{cases} -1 & , \text{if } \sigma'_{n,g}(Ur) \geq \sigma'_{n,g}(Lr) \text{ and } d(T_{n,g}) = 0 \\ 1 & , \text{if } \sigma'_{n,g}(Ur) < \sigma'_{n,g}(Lr) \text{ and } d(T_{n,g}) = 0 \end{cases} \\ D[T'_{n,g}] &= \begin{cases} -1 & , \text{if } \sigma'_{n,g}(Lt) \geq \sigma'_{n,g}(Rt) \text{ and } d(T_{n,g}) = 1 \\ 1 & , \text{if } \sigma'_{n,g}(Lt) < \sigma'_{n,g}(Rt) \text{ and } d(T_{n,g}) = 1 \end{cases} \\ D[T'_{n,g}] &= \begin{cases} -1 & , \text{if } \sigma'_{n,g}(D_1) \geq \sigma'_{n,g}(D_2) \text{ and } d(T_{n,g}) = 2 \\ 1 & , \text{if } \sigma'_{n,g}(D_1) < \sigma'_{n,g}(D_2) \text{ and } d(T_{n,g}) = 2 \end{cases} \end{aligned} \quad (18)$$

From multi-resolution transform point of view, the location of watermarked coefficients in different wavelet level will play different importance during the image reconstruction. Therefore, the watermarked bits extracted from 6 blocks in each tree can not be treated equally during the watermark bit verification. How to get the appropriate weighting is another issue needed to be addressed.

Since the sensitivity of human vision is different from various spatial frequencies (frequency subbands), the HVS (Human Visual System) study is the key factor to provide a better understanding of visual effect and the imperceptibility of the watermarked image. For that reason, the watermarked coefficients of different wavelet level will affect the contrast sensitivity. Therefore, DEED has adopted the contrast sensitivity function (CSF) of the HVS from [7] to determine the accurate weighing values for different wavelet levels.

For watermarked images, there has been a need for good metrics for image quality that incorporates properties of the HVS. The visibility thresholds of visual signals are studied by psychovisual measurements to determine the thresholds. These measurements were performed on sinusoidal gratings with various spatial frequencies and orientations by given viewing conditions. The purpose of such study was to determine the contrast thresholds of gratings by the given frequency and orientation. Contrast as a measure of relative variation of luminance for periodic pattern such as a sinusoidal grating is given by the equation

$$C = (L_{\max} - L_{\min}) / (L_{\max} + L_{\min}) \quad (19)$$

where L_{\max} and L_{\min} are maximal and minimal luminance of a grating. Reciprocal values of contrast thresholds express the contrast sensitivity (CS), and Mannos and Sakrison [11] originally presented a model of the contrast sensitive function (CSF) for luminance (or grayscale) images is given as follows:

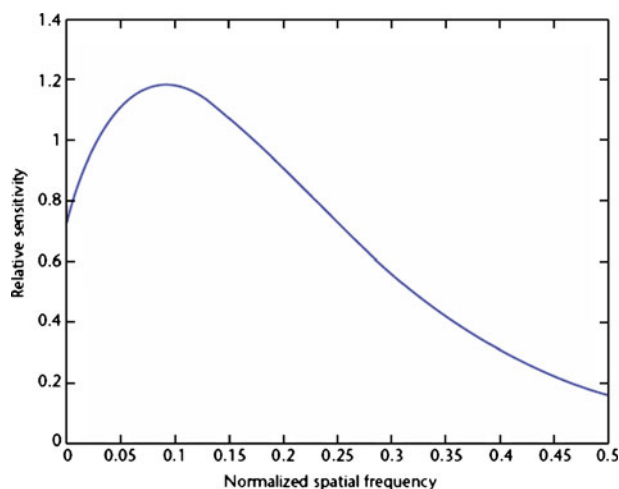
$$H(f) = 2.6 * (0.0192 + 0.114 * f) * e^{-(0.114 * f)^{1.1}} \quad (20)$$

where $f = \sqrt{f_x^2 + f_y^2}$ is the spatial frequency in cycles/degree of visual angle (f_x and f_y are the spatial frequencies in the horizontal and vertical directions, respectively). Figure 3 depicts the CSF curve which characterizes luminance sensitivity of the HVS as a function of normalized spatial frequency and the knowledge from CSF can be used to develop a HVS dependent model. Therefore, CSF masking [2, 7, 11, 14, 15, 20] is one way to apply the CSF in the discrete wavelet domain. CSF masking refers to the method of weighting the wavelet coefficients according to their perceptual importance. To apply the CSF in the DWT domain, CSF masking is employed and refers to the method of weighting the wavelet coefficients relative to their perceptual importance [14, 15]. The weights of wavelet coefficient under CSF perceptual importance are shown for each subband in Fig. 1.

If the wavelet tree is constructed by coefficients in HL or LH subband, the judgment value w'_n is determined as follows:

$$w'_n = D[T'_n(1)] \times 3.55 + D[T'_{n,1}] \times 5.3 + (D[T'_{n,2}] + D[T'_{n,3}] + D[T'_{n,4}] + D[T'_{n,5}]) \times 4.74 \quad (21a)$$

Fig. 3 Luminance CSF [7]



If the wavelet tree is constructed by coefficients in HH subband, the judgment value w_n is determined as follows:

$$w_n' = D[T_n'(1)] \times 3.48 + D[T_{n,1}'] \times 7.2 + (D[T_{n,2}'] + D[T_{n,3}'] + D[T_{n,4}'] + D[T_{n,5}']) \times 3.75 \quad (21b)$$

Finally we will get the extracted watermark bit w_n'' from w_n' as follows:

$$W_n'' = \begin{cases} -1, & w_n' \geq 0 \\ 1, & w_n' < 0 \end{cases} \quad (22)$$

To quantify the existence of the watermark after all watermark bits are extracted from the decoder, the normalized correlation (NC) coefficient [3] will be examined in order to identify the existence of the watermark. The formula of normalized correlation coefficient is as follows:

$$\rho(W, W'') = \frac{\sum_{n=1}^{N_w} w_n w_n''}{\sqrt{\sum_{n=1}^{N_w} w_n^2 \sum_{n=1}^{N_w} w_n'^2}} = \frac{\sum_{n=1}^{N_w} w_n w_n''}{N_w} \quad (23)$$

The coefficient value is within -1 and 1 . The existence decision is “yes” if $\rho(W, W'') \geq \rho_T$ and “no” if $\rho(W, W'') < \rho_T$. The threshold ρ_T is chosen based on the probability of false positive error P_{fp} which is computed by [8]:

$$P_{fp} = \sum_{n=\lceil N_w \times (\rho_T + 1) / 2 \rceil}^{N_w} \binom{N_w}{n} P_E^{N_w - n} \cdot (1 - P_E)^n \quad (24)$$

The estimation of the probability of a false positive (i.e., false watermark detection) is analyzed as following [8]:

We define the probability of false watermark detection as

$$P_{fp} = P\{\rho(W, \tilde{W}) \geq \rho_T | \text{no watermark}\} \quad (25)$$

where $P\{A|B\}$ is the probability of event A given event B , W is the given watermark and \tilde{W} is the extracted one. Since $W(n)$ and $\tilde{W}(n)$ are either one or negative one, and subsequently $W^2(n) = \tilde{W}^2(n) = 1$. Let P_E be the probability of bit error during extraction. A bit error occurs when $\tilde{W}(n) \neq W(n)$ or more specifically, when $\tilde{W}(n) = -W(n)$ (since $W(n), \tilde{W}(n) \in \{-1, 1\}$). If we let $k(n) = W(n) \cdot \tilde{W}(n)$, then $k(n) = -1$ indicates a bit error and $k(n) = 1$ indicates no error. We may rewrite the expressions for ρ and P_{fp} in terms of $k(n)$ as

$$\rho(W, \tilde{W}) = \frac{\sum_{n=1}^{N_w} W(n) \tilde{W}(n)}{N_w} = \frac{\sum_{n=1}^{N_w} k(n)}{N_w} \quad (26)$$

and

$$P_{fp} = P\left\{\sum_{n=1}^{N_w} k(n) \geq N_w \rho_T | \text{no watermark}\right\}, \quad (27)$$

Since $k(n) \in \{-1, 1\}$, it can be shown that $\sum k(n)$ must take on discrete values from the set $\{-N_w, -N_w + 2, -N_w + 4, \dots, N_w - 4, N_w - 2, N_w\}$, or $\sum k(n) = -N_w + 2m$, where $m=0, 1, \dots, N_w$. Thus, we find that

$$\begin{aligned} P_{fp} &= P\left\{\sum_{n=1}^{N_w} k(n) \geq N_w \rho_T \mid \text{no watermark}\right\} \\ &= \sum_{m=\lceil N_w(\rho_T+1)/2 \rceil}^{N_w} P\{\sum k(n) = -N_w + 2m \mid \text{no watermark}\}, \end{aligned} \quad (28)$$

Where $P\{\sum k(n) = -N_w + 2m \mid \text{no watermark}\}$ is the probability that the series $\{k(n)\}$ contains m ones and $N_w - m$ negative ones. Since $\sum k(n) = -N_w + 2m \geq N_w \rho_T$ and $2m \geq N_w \rho_T + N_w$, m 's range is from $\lceil N_w(\rho_T + 1)/2 \rceil$ to N_w . Therefore,

$$P\left\{\sum k(n) = -N_w + 2m \mid \text{no watermark}\right\} = \binom{N_w}{m} P_E^{N_w-m} \cdot (1 - P_E)^m \quad (29)$$

Where P_E is the probability that $k(n) = -1$ and $\binom{N_w}{m} = \frac{N_w!}{m!(N_w-m)!}$. Since we are given that no watermark is embedded, we can assume that extracted mark \tilde{W} consists of a series of random independent equally probable values from the set $\{-1, 1\}$. Thus, $P_E = 0.5$. Substituting into Eqs. 28 and 29,

$$P_{fp} = \sum_{m=\lceil N_w(\rho_T+1)/2 \rceil}^{N_w} \binom{N_w}{m} 0.5^{N_w}. \quad (30)$$

Given the reasonable assumption, $P_E = 0.5$ and $N_w = 512$ as the watermark length, P_{fp} will be as low as 4.5×10^{-4} , 3.86×10^{-6} and 8.45×10^{-9} while $\rho_T = 0.15, 0.20$ and 0.25 respectively. That means the appropriate ρ_T will be selected to meet the requirement given a false positive probability.

2.3 The complete algorithms of DEED

The complete design of the proposed algorithm is summarized as following:

2.3.1 DEED watermark embedding

- 1) Generate a seed by mapping a signature/text through a one-way deterministic function. Obtain a PN sequence W of length N_w using the seed k .
- 2) Compute wavelet coefficients of a host image. Group the coefficients to form trees.
- 3) Randomly arrange the trees using some pseudorandom generator and each tree is divided into 6 blocks. The block 1 has 1 coefficient in level 4 and block 2–6 has 4 coefficients in level 2 or level 3. The coefficient of block 1 in T_n is represented as $T_n(1)$ and the j th coefficient of block 2–6 is represented as $T_{n,g}(j)$ for $g=1$ to 5.
- 4) FOR EACH watermark bit w_n ($n=0$ to $N_w - 1$) DO
 - a) Select the modular value S and calculate the $T_n(1)$ with Eq. 1, 2.
 - b) Find the suitable differentiation direction of $T_{n,g}$ for $g=1$ to 5 from Eq. 3 and modify the energy with Eq. 4–7 if direction is vertical, Eq. 8–10, 14 if direction is

horizontal, and Eq. 11–13, 15 if direction is diagonal. A random number generator using the seed k will be applied to select certain groups to embed watermark bit w_n and the others to embed $-w_n$. The information of differentiation direction list for each tree blocks will be kept as a secret key.

- c) Record the differentiation direction of $T_{n,g}$
- 5) Arrange back the modulated trees to their original positions.
- 6) Pass the modified wavelet coefficients through the inverse DWT to obtain a watermarked image.

2.3.2 Note

- 1) The watermark W is a binary PN sequence of ± 1 .
- 2) The maximal length of watermark=the number of trees. If the test image is 512×512 , the maximum length of the watermark=3072.

2.3.3 DEED watermark extraction

- 1) Generate a seed by mapping a signature/text through a one-way deterministic function. Obtain a PN sequence W of length N_w using the seed k .
- 2) Compute wavelet coefficients of a host image. Group the coefficients to form trees and arrange the trees using the same generator and the private key for the information of differentiation direction list.
- 3) FOR EACH watermark bit w_n ($n=0$ to $N_w - 1$) DO
 - a) Using modular value S and $T_n'(1)$ to calculate the $D[T_{n,g}'(1)]$ with Eq. 16, 17
 - b) Get the differentiation directions of $T_{n,g}'$ and determine the $D[T_{n,g}']$ with (18) for $g=1$ to 5. If $-w_n$ has been embedding for certain group g , $D[T_{n,g}'] = -D[T_{n,g}']$
 - c) Calculate the judgment value w_n' by (21a) and (21b). IF ($w_n' \geq 0$) THEN $w_n'' = 1$ ELSE $w_n'' = -1$
- 4) Compute the normalized correlation ρ .
- 5) If ρ is above the threshold ρ_T , the watermark W exists; otherwise, it does not exist.

2.4 DEED_R watermarking

Since the information of differentiation direction list must be kept secret which addresses extra storage space is needed, DEED may be categorized as a non-blind watermarking scheme. Therefore, DEED has the weakness that if the differentiation direction information is lost or damaged, we could not calculate the value of extracted watermark bit w_n'' .

In view of this, we propose a revised method to make DEED more flexible. Since we use some pseudorandom generator to randomly arrange the trees in step (3) of DEED watermark embedding procedure, we can obtain the order value of each tree. Then we can use the order value of each tree as a new pseudorandom generator to

enforce the random direction of this tree and it is called DEED_R (R means random direction differentiation).

The pseudo code procedures are as follows:

```

for ( n=0 ; n<Nw ; n++ )
{
    srand ( n )

    for ( g=1 ; g<=5 ; g++ )

    {
        i = ( rand() % 3 )

        if      ( i = 0 )      d(Tn,g) = vertical
        else if ( i = 1 )      d(Tn,g) = horizontal
        else if ( i = 2 )      d(Tn,g) = diagonal
    }
}

```

Where $d(T_{n,g})$ is the differentiation direction of the g th block in tree T_n .

In the mean time, the random number generator applied in step (4) of DEED watermark embedding procedure will be applied for DEED_R to select which group will embed the watermark bit w_n and the others will embed $-w_n$ for each tree T_n in order to counteract the cryptanalysis attack for DEED_R.

During the watermark extraction step, we can use the same way to determine the differentiation direction of each block in each tree from the order value of each tree that the trees are arranged using the same pseudorandom generator. Therefore, the DEED_R algorithm is then designed which doesn't need the extra information for watermark extraction, and DEED_R is a truly blind watermarking scheme.

The complete design of DEED_R embedding and extraction is summarized as following:

2.4.1 DEED_R watermark embedding

- 1) Same procedures of steps (1)–(3) from **DEED Watermark Embedding**.
- 2) FOR EACH watermark bit w_n ($n=0$ to $N_w - 1$) DO
 - a) Select the modular value S and calculate the T_n (1) with Eq. 1, 2.
 - b) Use the order value n as a seed to generate a random value and make this value divided by 3 to determine the forced differentiation direction of $T_{n,g}$ for $g=1$ to 5 as shown in Eg. (25).
 - c) Modify the energy with Eq. 4–7 if direction is vertical, Eq. 8–10, 14 if direction is horizontal, and Eq. 11–13, 15 if direction is diagonal. A random number generator based on the seed k will be applied to select certain groups to embed watermark bit w_n and the others to embed $-w_n$.

3) Same procedures of steps (5)–(6) from **DEED Watermark Embedding**.

2.4.2 $DEED_R$ watermark extraction

- 1) Same procedures of steps (1) from **DEED Watermark Extraction**.
- 2) Compute wavelet coefficients of a host image. Group the coefficients to form trees and arrange the trees using the same generator.
- 3) FOR EACH watermark bit w_n ($n=0$ to $N_w - 1$) DO
 - a) Using modular value S and $T'_n(1)$ to calculate the $D[T'_n(1)]$ with Eq. 16, 17.
 - b) Use the order value n as a seed to generate a random value and make this value divided by 3 to get the forced differentiation direction of $T'_{n,g}$. for $g=1$ to 5.
 - c) Apply Eq. 18 to determine the $D[T'_{n,g}]$. If $-w_n$ has been embedding for certain groups, $D[T'_{n,g}] = -D[T'_{n,g}]$.
 - d) Calculate the judgment value w'_n by (21a) and (21b). IF ($w'_n \geq 0$) THEN $w''_n = 1$ ELSE $w''_n = -1$
- 4) Same procedures of steps (4)–(5) from **DEED Watermark Extraction**.

3 Experiments and discussion

To evaluate the performance of the proposed method, the 512×512 Lena, Goldhill and Peppers images with 8 bits/pixel resolution are used for watermarking. In order to make the fair comparison, all the watermarked images will be set at the same PSNR values shown as in [19] of WTQ algorithm since it is the typically representative wavelet tree based approach. The wavelet filters used in this study for the wavelet tree watermarking is the CDF 9/7 filters [6] which are also used in WTQ. We employ a four-level wavelet transform and a watermark sequence of length 512. In order to compare the performance with the WTQ and WTGM schemes, Lena, Goldhill and Peppers are set at the same PSNR values of 38.2, 38.7 and 39.8 dB from [19] respectively while S of Eq. 1 is set at 48 and Δ applied in Eq. 7, 14, 15 is equal to 10. With watermark length $N_w=512$, the threshold ρ_T is chosen to be 0.23 for a false positive probability of 1.03×10^{-7} . All the results from common image processing attacks, geometric attacks and security measure are tabulated in Table 1(a), (b) and (c) respectively for Lena, Goldhill and Peppers. Those attacks are selected based on the fact that WTQ has tabulated in [19] so we can make the fair comparison. In addition, WTGM considers the tree grouping information globally but ABW-TMD only locally and the listed results from ABW-TMD is not as good as WTGM [16, 17]. Therefore, we will only compare DEED, $DEED_R$ with WTGM and WTQ in this study.

3.1 Common image processing attacks

1) JPEG Compression Attacks

In this experiment, we perform JPEG compression with different quality factors (QF) on the watermarked image. The extracted results and NC values are depicted in Table 1. Figure 4(a, b) illustrate the JPEG compressed Lena image for visual comparison. From these results, we can see that the proposed algorithm for DEED and $DEED_R$ is robust to

JPEG compression. For all cases, the extracted watermarks are with relatively high-NC values and the results are also better than two settings of WTGM(S_1) and WTGM(S_2). Even for the case that QF is equal to 30, we can still detect the embedded watermark but WTQ is failed for Lena and Goldhill image.

2) SPIHT Compression Attacks

SPIHT (Set Partitioning in Hierarchical Trees) [12] is an image compression algorithm that exploits the inherent similarities across subbands in a wavelet decomposition of an image. It implies uniform quantization and bit allocation applied after wavelet decomposition. Table 1 shows the extracted NC values and corresponding PSNR values between original image and attacked image. From these results, we can see that the proposed algorithm can tolerate the incidental distortions induced by high-quality SPIHT compression. The performance of DEED and DEED_R is still better than WTGM for the testing images.

3) Spatial-Domain Image Processing Attacks

Several spatial-domain image processing techniques, including median filtering, Gaussian filtering and sharpening performed on the watermarked image and the results are also shown in Table 1. Figure 4(c) shows a medium filter attacked image for visual result. For all cases, DEED and DEED_R algorithms outperform the WTQ scheme with high normalized correlation values in all cases and watermark information therein can be successfully recognized. In addition, DEED based methods are comparable with WTGM for all cases.

3.2 Geometric attacks

1) Pixel Shifting Attacks (Circular Shift)

This kind of attacks is done by shifting the pixels circularly. Here, we shift the pixels to the left. From Table 1, DEED based algorithms can detect the watermark but WTGM(S_1) is unable to resist such attack for Lena and Peppers images.

2) Rotation Attacks (Rotation and Scaling)

The attack is done by rotating the image by a small angle, scaling the rotated image, and cropping the scaled image to the original image size. StirMark [13] software is adopted here for this attack since it provides the described testing functions. This rotation and scaling is a geometrical attack in the spatial domain and an illustration of the operation is demonstrated in Fig. 5. From Table 1, WTGM has better performance than DEED based algorithms but they all outperform WTQ while the rotation degree is up to 0.75°.

Regarding the geometric attacks, WTGM(S_2) performs well and it is necessary to discuss its characteristics. WTGM(S_1) uses coefficient number 1~21 corresponding to relatively low-frequency components (level 2, 3 and 4 of DWT in Fig. 1) for watermarking, which is the same as the WTQ and DEED schemes. On the other hand, WTGM(S_2) uses coefficient number 6~85 corresponding to relatively high-frequency components (level 1 and 2 of DWT in Fig. 1). Therefore, WTGM(S_1) can be more effective in resisting JPEG and SPIHT compression but WTGM(S_2) with medium-high frequency setting is superior to resist geometric distortion. Even DEED still performs better than WTGM(S_1), it is the future research for DEED to adopt S_2 settings and verify whether it can improve its capability for geometric attacks while more high frequency components are associated with watermark

Table 1 Performance summary of DEED, DEED_R, WTGM(S_1), WTGM(S_2) and WTQ schemes for (a) LENA (b) Goldhill and (c) Peppers images

	Operations	DEED	DEED _R	WTGM(S_1)	WTGM(S_2)	WTQ
(a)						
[Signal Processing Attacks]						
JPEG (QF=90%)	1.00	1.00	1.00	1.00	1.00	1.00
JPEG (QF=50%)	1.00	1.00	0.98	0.94	0.94	0.26
JPEG (QF=30%)	1.00	1.00	0.94	0.77	0.77	0.15
SPIHT (bitrate=0.7)	1.00	1.00	1.00	1.00	1.00	0.85
SPIHT (bitrate=0.5)	1.00	1.00	0.99	0.99	0.99	0.85
SPIHT (bitrate=0.3)	1.00	0.93	0.96	0.77	0.77	0.21
Median Filtering (4×4)	0.94	0.86	0.56	0.57	0.57	0.23
Gaussian Filtering	0.72	0.59	0.46	0.68	0.68	0.64
Sharpening	0.98	0.98	0.63	1.00	1.00	0.46
[Geometric Attacks]						
Pixel Shifting (6 pixels)	0.23	0.24	0.14	0.89	0.89	0.34
Rotation (0.75°)	0.36	0.27	0.33	0.90	0.90	0.26
[Security Measurement]						
Multiple Watermarking (4 watermarks)	1.00 (31.3dB)	0.67 (31.1dB)	0.62 (31.52dB)	0.59 (26.81dB)	0.59 (26.81dB)	0.11 (28.05 dB)
Multiple Watermarking (8 watermarks)	1.00 (29.4dB)	0.56 (29.2dB)	0.15 (24.46dB)	0.73 (29.81dB)	0.73 (29.81dB)	N/A
Bitplane Removal (5 bitplanes)	0.98 (33.6dB)	0.88 (33.2dB)	0.78 (32.74dB)	0.88 (33.52dB)	0.88 (33.52dB)	0.11 (18.47 dB)
(b)						
[Signal Processing Attacks]						
JPEG (QF=90%)	1.00	1.00	1.000	1.00	1.00	1.00
JPEG (QF=50%)	1.00	1.00	0.99	0.99	0.99	0.71
JPEG (QF=30%)	1.00	1.00	0.95	0.92	0.92	0.23
SPIHT (bitrate=0.7)	1.00	1.00	1.00	1.00	1.00	0.35
SPIHT (bitrate=0.5)	1.00	0.98	0.99	0.97	0.97	0.23

[Geometric Attacks]	SPIHT (bitrate=0.3)	0.99	0.88	0.94	0.87	-0.06
	Median Filtering (4×4)	0.94	0.85	0.65	0.52	0.24
	Gaussian Filtering	0.80	0.75	0.58	0.80	0.56
	Sharpening	0.99	0.98	0.79	1.00	0.39
[Security Measurement]	Pixel Shifting (6 pixels)	0.27	0.26	0.28	0.90	0.35
	Rotation (0.75°)	0.33	0.28	0.43	0.89	0.21
	Multiple Watermarking (4 watermarks)	1.00 (31.9dB)	0.71 (31.5dB)	0.74 (31.24dB)	0.71 (29.87dB)	0.18 (28.57dB)
	Multiple Watermarking (8 watermarks)	1.00 (30.0dB)	0.58 (29.7dB)	0.14 (24.58dB)	0.20 (28.28dB)	N/A
(c)	Biplane Removal (5 bitplanes)	1.00 (32.2dB)	0.84 (31.9dB)	0.93 (31.7dB)	0.88 (31.21dB)	0.14 (16.18dB)
	[Signal Processing Attacks]					
	JPEG (QF=30%)	1.00	1.00	1.00	1.00	1.00
	JPEG (QF=50%)	1.00	1.00	0.94	0.63	0.70
[Geometric Attacks]	JPEG (QF=30%)	1.00	0.99	0.83	0.49	0.34
	SPIHT (bitrate=0.7)	1.00	1.00	0.98	1.00	0.85
	SPIHT (bitrate=0.5)	1.00	1.00	0.99	0.98	0.65
	SPIHT (bitrate=0.3)	0.99	0.92	0.93	0.64	0.36
[Security Measurement]	Median Filtering (4×4)	0.96	0.91	0.56	0.40	0.25
	Gaussian Filtering	0.71	0.67	0.36	0.42	0.74
	Sharpening	1.00	0.98	0.55	0.99	0.62
	Pixel Shifting (6 pixels)	0.29	0.25	0.18	0.86	0.34
(c)	Rotation (0.75°)	0.28	0.23	0.27	0.81	0.26
	Multiple Watermarking (4 watermarks)	1.00 (32.8 dB)	0.73 (32.37 dB)	0.75 (32.45dB)	0.64 (29.96dB)	0.22 (28.81 dB)
	Multiple Watermarking (8 watermarks)	1.00 (30.87 dB)	0.57 (30.52 dB)	0.22 (24.41dB)	0.40 (29.18dB)	N/A
	Biplane Removal (5 bitplanes)	0.98 (33.98 dB)	0.49 (33.66 dB)	0.73 (33.42dB)	0.59 (33.39dB)	0.14 (16.93 dB)



Fig. 4 **a** Original watermarked Lena image by DEED_R **b** JPEG compressed Lena image with QF=40%, PSNR=33.49dB and $\rho=1$ **c** 4×4 Median Filter attacked Lena image with $\rho=0.86$ **d** The attacked Lena image where 5 lowest bitplanes in the wavelet domain are removed. PSNR=33.2dB, $\rho=0.88$

embedding. On the other hand, it is for sure that S_2 settings for DEED will dramatically increase its complexity.

3.3 Security measurement

1) Multiple Watermarking

For algorithms well-known to all, the attacker may apply one or more watermarks using the same wavelet tree group modulation technique in an attempt to disturb the detector or to destroy the embedded watermark. Figure 6 shows an illustration of Goldhill image which is inserted by 5 watermarks. More watermarks are in the image, more image quality will be affected. However, DEED based algorithms achieve high correlation values for multiple watermark attacks. From Table 1, DEED and DEED_R have superior performance than WTGM and WTQ for up to 8 multiple watermarks.

2) Bitplane Removal

Bitplane removal is one of the major strategies used to defeat the WTQ scheme. We perform this attack designated on the embedded subbands, which reduces the impact on watermarked images. Figure 4(d) shows an illustration of Lena image where 5 lowest



Fig. 5 An illustration of rotation and scaling attack for the Goldhill image. **a** counter clockwise rotation and scaling **b** clockwise rotation and scaling

bitplanes in the wavelet domain are removed. Table 1 shows that the DEED based algorithms and WTGM can resist 5 bitplanes removed but WTQ can not.

3.4 Complexity of DEED with human vision system

The computation complexity of DEED is low from the view of mathematical analysis. The whole complexity should be discussed for wavelet transform, CSF and decision calculation respectively.

Suppose the synthesis filters are h (low-pass) and g (high-pass) for wavelet transform. Take $|h|=2N$, $|g|=2M$, and assume $M \geq N$. The cost of the standard algorithm for CDF 9/7 filters is $4(N+M)+2$ and could be speeded up by the lifting algorithm in [6] to $2(N+M+2)$. The computation of wavelet transform is linear time mathematics.

On the other hand, CSF masking is employed to apply the CSF in the DWT domain and the associated perceptual weighting function can be pre-calculated for each subband as shown in Fig. 1. Therefore, the complexity of CSF implementation in DEED becomes the coefficient multiplication from the look-up table. This can be efficiently done in linear-time.

The watermark decision procedure for Eq. 4–15 and Eq. 16–21b is pure add, subtract and comparison which can be done in linear time. From our simulation, the whole loop of

Fig. 6 **a** Original Goldhill image **b** 5 watermarks are inserted into Goldhill by DEED. PSNR=30.80dB and $\rho=1$



DEED and $DEED_R$ embedding and extraction under Intel Pentium 3.2G Hz, 1G RAM desktop computer will need less than 1 s to complete for 512×512 testing images.

Unlike the group strategy of sum-of-subsets in WTGM, it is essentially a known NP-complete problem [5]. Therefore, its complexity is higher than DEED and $DEED_R$. In conclusion, the DEED and $DEED_R$ complexity is low and suitable for practical applications based on the mathematical analysis and simulation results.

3.5 Summary

DEED, $DEED_R$ and WTGM algorithms apply the positive and negative modulation to embed the watermark within the trees. Therefore, the cryptanalysis-like attack for WTQ is not useful to remove the watermark for DEED and WTGM. From the outcomes in Table 1, the tabulated results also disclose DEED and $DEED_R$ are superior to WTGM and WTQ in almost all categories with significant high PSNR values. Since high PSNR has positive correlation with better image quality, the CSF human visual system applied in DEED and $DEED_R$ shows accurate weighting and visual characteristics.

In fact, DEED utilizes the best coefficient energy differentiation direction of the embedded watermark bit that makes minimal change of coefficient's energy within the tree. However, the weakness of DEED is that the differentiation direction information should be recorded and extra storage of side information is required as the WTGM or ABW-TMD does, it can not be categorized as the blind watermarking approach which will be unsuitable in practical applications. In addition, non-blind watermarking can essentially perform better than non-blind schemes since extra information can be preserved in the side information. There are apparent results from Table 1 where non-blind schemes like DEED, WTGM perform better than WTQ. Since such kind of comparison is not fair, a random direction differentiation approach called $DEED_R$ is then devised which is a truly blind watermarking technique with high robustness against attacks. In summary, DEED is better than $DEED_R$ since random direction differentiation doesn't guarantee the best choice among selections.

Nevertheless, there are vulnerabilities for DEED and WTGM. For example, DEED needs to record the tree structure and the modulation direction information where WTGM must keep the tree combination information secret which addresses extra storage space. Even it is possible to design a random grouping approach for WTGM, the affected coefficients will be significant (whole tree instead of blocks in DEED) and results very low image quality. The extended study should work on the design to efficiently reduce this extra cost. At the present time, $DEED_R$ is the best choice since it doesn't need the side information during the watermark extraction which is the truly blind watermarking approach.

In this study, we focus on the same decomposition structure for different wavelet tree watermarking algorithms. On the other hand, it is also possible to consider different decomposition level for DEED. For most of the wavelet tree watermarking architecture, it is pretty common to adopt 4 levels of decomposition (the S_1 setting as shown in Fig. 1) which results only one coefficient existing in the Level 4 as shown in Fig. 1 for 512×512 images. Therefore, four level wavelet decomposition is the maximum possible decomposition structure for 512×512 images and DEED with $DEED_R$ can only apply quantization approach to embed the watermark bit since there is one component left for embedding. For coefficients located at other levels, there are enough components (at least 4 coefficients) to choose the differentiation direction for watermark embedding. In the manner of alternatives, fewer level of wavelet decomposition has been discussed in Section 3.2 where WTGM(S_2) format (coefficients in level 1 and level 2) are investigated for watermark embedding. From experimental results of Table 1, it is clear such decomposition structure for WTGM can

have better robustness against pixel shifting, rotation of geometric attacks even it is less resistant to JPEG, SPIHT compression and multiple watermarking attacks. The reason is apparent since more medium-high frequency components in S_2 are adopted for watermark embedding compared with the setting of S_1 . Even it is the future study for DEED to adopt S_2 settings and verify whether it can improve its capability for geometric attacks while more high frequency components are associated with watermark embedding, the results can be predicted based on the previous studies of WTGM that S_2 settings for DEED will dramatically increase its complexity.

In addition, the maximum length of the watermark for DEED based algorithm is 3072 for the 512×512 image but the maximum length of the watermark for WTGM and ABW-TMD is 1536. On the other hand, the maximum length of the watermark for WTQ is only 768. Therefore, we can find the DEED based algorithms can contain much longer watermark bit length which increases the security level in practical applications.

4 Conclusion

The human vision system based tree energy differentiation (DEED) watermarking algorithms have been presented in this study. Compared with other watermarking schemes like WTGM and WTQ, the proposed algorithm can tolerate more common signal processing and geometric attacks. In addition, the human visual characteristics are considered for better performance in watermark extraction. Regarding the cryptanalysis of the algorithm, the algorithm can be public with the keys remained private for DEED and totally blind detection for DEED_R algorithm.

Compared with the WTGM, ABW-TMD and WTQ scheme, the advantages of the proposed DEED algorithms are as follows:

- 1) The proposed algorithm can tolerate more common signal processing and geometric attacks with superior performance.
- 2) The length of the image key is large, which renders a better confusion/diffusion for security.
- 3) The human visual characteristics are considered in the wavelet tree watermarking systems to provide the better visual quality.

Acknowledgments The author would like to thank the anonymous reviewers with their valuable comments to improve the quality of this manuscript and Bai-Jiun Chen at National Chiao Tung University who helps to write the programs for software experiments. This work is partially supported by the National Science Council in Taiwan, Republic of China, under Grant NSC96-2416-H009-015, NSC97-2410-H009-034 and 99-2918-1-009-008.

References

1. Al-Otum HM, Samara NA (2006) Adaptive blind wavelet-based watermarking technique using tree mutual differences. *J Electron Imaging* 15(4):043011
2. Beegan AP, Iyer LR, Bell AE (2002) Design and evaluation of perceptual masks for wavelet image compression. *Proc. 10th IEEE Digital Signal Processing Workshop*, pp. 88–93
3. Cox IJ, Kilian J, Leighton FT, Shamoon T (1997) Secure spread spectrum watermarking for multimedia. *IEEE Trans on Image Proc* 6(12):1673–1687
4. Das TK, Maitra S (2004) Cryptanalysis of wavelet tree quantization watermarking scheme. *IWDC 2004*:219–230
5. Das TK, Maitra S, Mitra J (2005) Cryptanalysis of optimal differential energy watermarking (DEW) and a modified robust scheme. *IEEE Trans on Signal Proc* 53(2):768–775

6. Daubechies I, Sweldens W (1998) Factoring wavelet transforms into lifting steps. *J Fourier Anal Appl* 4(3):247–269
7. Huang BB, Tang SX (2006) A contrast-sensitive visible watermarking scheme. *IEEE Multimedia* 13(2):60–66
8. Kundur D, Hatzinakos D (1998) Digital watermarking using multiresolution wavelet decomposition. *Proc IEEE ICASSP* 5:2869–2972
9. Langelaar GC, Lagendijk RL (2001) Optimal differential energy watermarking of DCT encoded images and video. *IEEE Trans on Image Proc* 10(1):148–158
10. Lu CS, Huang SK, Sze CJ, Liao HY (2000) Cocktail watermarking for digital image protection. *IEEE Trans on Multimedia* 2(4):209–224
11. Mannos JL, Sakrison DJ (1974) The effects of a visual fidelity criterion on the encoding of images. *IEEE Trans on Info Theory* 20(4):525–536
12. Said A, Pearlman WA (1996) A new, fast, and efficient image codec based on set partitioning in hierarchical trees. *IEEE Trans Circuits Syst Video Technol* 6:243–250
13. StirMark, [Online]: http://www.petitcolas.net/fabien/software/StirMarkBenchmark_4_0_129.zip
14. Tsai M-J (2009) A visible watermarking algorithm based on the content and contrast aware (COCOA) technique. *J Vis Commun Image Represent* 20(5):323–338
15. Tsai MJ, Lin CW (2008) Wavelet based multipurpose color image watermarking by using dual watermarks with human vision system models. *IEICE E91-A(6)*:1426–1437
16. Tsai MJ, Shen CH (2007) Wavelet Tree Group Modulation (WTGM) for digital image watermarking. *IEEE ICASSP2007* 2:173–176
17. Tsai MJ, Shen CH (2008) Differential energy based watermarking algorithm using Wavelet Tree Group Modulation (WTGM) and human visual system. *IEICE E91-A(8)*:1961–1973
18. Wang SH, Lin YP (2002) Blind watermarking using wavelet tree quantization. *IEEE International Conference on Multimedia and Expo* 1:589–592
19. Wang SH, Lin YP (2004) Wavelet tree quantization for copyright protection watermarking. *IEEE Trans on Image Proc* 13(2):154–165
20. Yong L, Cheng LZ, Xu ZH (2004) Translucent digital watermark based on wavelets and error-correct code. *Chinese J of Computers* 20(11):1533–1539



Min-Jen Tsai received the B.S. degree in electrical engineering from National Taiwan University in 1987, the M.S. degree in industrial engineering and operations research from University of California at Berkeley in 1991, the engineer and Ph.D. degrees in Electrical Engineering from University of California at Los Angeles in 1993 and 1996, respectively. He served as a second lieutenant in Taiwan army from 1987 to 1989. From 1996 to 1997, he was a senior researcher at America Online Inc. In 1997, he joined the institute of information management at the National Chiao Tung University in Taiwan and is currently an associate professor. His research interests include multimedia system and applications, digital right management, digital watermarking and authentication, digital forensic, enterprise computing for electronic commerce applications. Dr. Tsai is a member of IEEE, ACM and Eta Kappa Nu.